Front. Optoelectron. 2012, 5(4): 351–357
DOI 10.1007/s12200-012-0294-6

REVIEW ARTICLE

Optical fiber amplifiers for space-division multiplexing

Dagong JIA (✉)[1,2,3], Haiwei ZHANG[1,2], Zhe JI[1,2], Neng BAI[3], Guifang LI (✉)[3]

1 College of Precision Instrument & Opto-electronics Engineering, Tianjin University, Tianjin 300072, China
2 Key Laboratory of Opto-electronics Information Technology of the Ministry of Education, Tianjin 300072, China
3 College of Optics & Photonics/CREOL&FPCE, University of Central Florida, 4000 Central Florida Boulevard, Orlando, Florida 32816-2700, USA

Abstract Recently, space-division multiplexing (SDM) techniques using multi-core fiber (MCF) and few-mode fiber (FMF) have been introduced into optical fiber communication to increase transmission capacity. Two main types of optical fiber amplifiers based on the Erbium-doped fiber (EDF) and the Raman effect have been developed to amplify signals in the MCF and FMF. In this paper, we reviewed the principles and configurations of these amplifiers.

Keywords optical fiber amplifier, space-division multiplexing (SDM), multi-core fiber (MCF), few-mode fiber (FMF)

1 Introduction

The transmission capacity of optical fiber links (single-core, single-mode fiber) is reaching its limitation. Without innovations in the physical infrastructure, optical transmission systems will soon face a "capacity crunch" [1]. To overcome this problem, a new multiplexing technique, namely, space-division multiplexing (SDM) using multi-core fibers (MCF) and few-mode fibers (FMF) has been proposed. The MCF is a fiber that consists of a number of independent single- (or multi-) mode cores [2–6]. The FMF is a fiber which has one core with sufficiently large cross-section area to support a number of independent guiding modes [7–9]. Experiments on SDM using MCFs or FMFs have demonstrated large capacity as well as long transmission distances [10].

It is well known that, when optical signals are transmitted along a single-mode fiber (SMF), inline fiber amplifiers are needed to compensate the transmission loss. Likewise, optical signals transmitted along a MCF or a FMF/multimode fiber (MMF) will also need inline optical amplification. Due to the lack of available inline amplifiers, most of the transmission experiments using MCF and MMF have been a single-span transmission with distance up to 76.8 km for MCF [11], 40 km [12] for MMF and 96 km for FMF [13]. So, suitable in-line optical amplifiers clearly need to be developed if SDM is to be used over longer transmission distances.

For single-mode transmission, inline fiber amplifiers are classified into three categories: amplifiers based on erbium-doped fiber, amplifiers based on stimulated Raman scattering (SRS) and amplifiers based on nonlinear refraction. The same types of amplification mechanisms can be applied to MCF and FMF. However, with additional degrees of freedom and the requirement to achieve high gain and high efficiency, and to control modal-dependent gain, the structures of MCF and FMF amplifiers are more complex than that of single-mode amplifiers. In this paper, we provide an overview of amplifiers for SDM. We evaluate the potential of the aforementioned concepts for MCF and MMF inline amplifier and analyze the differences between these amplifiers in term of the performance and efficiency.

2 Inline fiber amplifiers for SDM

2.1 Amplifiers based on Erbium-doped fibers

The principle of the Erbium-doped fiber amplifier (EDFA) was proposed in the early 1980s [14]. Since then single-mode EDFAs have been the preferred amplifiers in the majority of commercial long-haul systems. It is therefore desirable to extend the concept of single-mode EDFAs to MCF and FMF EDFAs. Up to now, several types of EDFAs have been proposed in recent report for SDM, such as multimode Erbium-doped fiber amplifier (MM-EDFA) [15–20], few-mode Erbium-doped fiber amplifier

Received September 18, 2012; accepted September 30, 2012

E-mail: dagongjia@tju.edu.cn, li@creol.ucf.edu

(FM-EDFA) [21] and multicore Erbium-doped fiber amplifier (MC-EDFA) [22].

2.1.1 FM-EDFA

It should be noted that the concept of multimode EDFA was proposed by Nykolak et al. in 1991 [23]. The application of the proposed MM-EDFA [23], however, was mainly used as a means of getting a high output power. Since the multimode optical fiber was essentially used in a "single mode" manner, the mode-dependent gain (MDG) is not critical. However, for mode-multiplexed transmission in SDM, careful control over MDG is necessary to overcome mode-dependent loss (MDL) during the optical amplification process, and to ensure all signal modes are launched with optimal power maximizing the total system capacity.

One of the ways to control MDG is to tailor the mode content of the pump as shown in Ref. [20]. The schematic and experimental setup of FM-EDFA is shown in Fig. 1. To generate the desired pump intensity profile, the pump source is split into N paths. Mode converters are used to transform the spatial mode of the pump source into the N spatial modes of the MMF. As shown in Fig. 1, free-space optics can be used for mode conversion method and phase plates are employed to convert modes between the pump and signals.

The operation of a multimode fiber amplifier can be described by a set of coupled differential equations, which includes the optical power evolution equation and the carrier population equation. The optical power evolution equations for the signal, amplified spontaneous emission (ASE) and the pumps are given by

$$\frac{\mathrm{d}P_{\mathrm{s},i}}{\mathrm{d}z} = P_{\mathrm{s},i}\int_0^{2\pi}\int_0^{a} r\mathrm{d}r\mathrm{d}\varphi\Gamma_{\mathrm{s},i}(r,\varphi)[N_2(r,\varphi,z)\sigma_{\mathrm{es},i} - N_1(r,\varphi,z)\sigma_{\mathrm{as},i}] - \sum_{k=1}^{m_{\mathrm{s}}} d_{\mathrm{s},i\leftrightarrow k}[P_{\mathrm{s},i} - P_{\mathrm{s},k}], \quad (1)$$

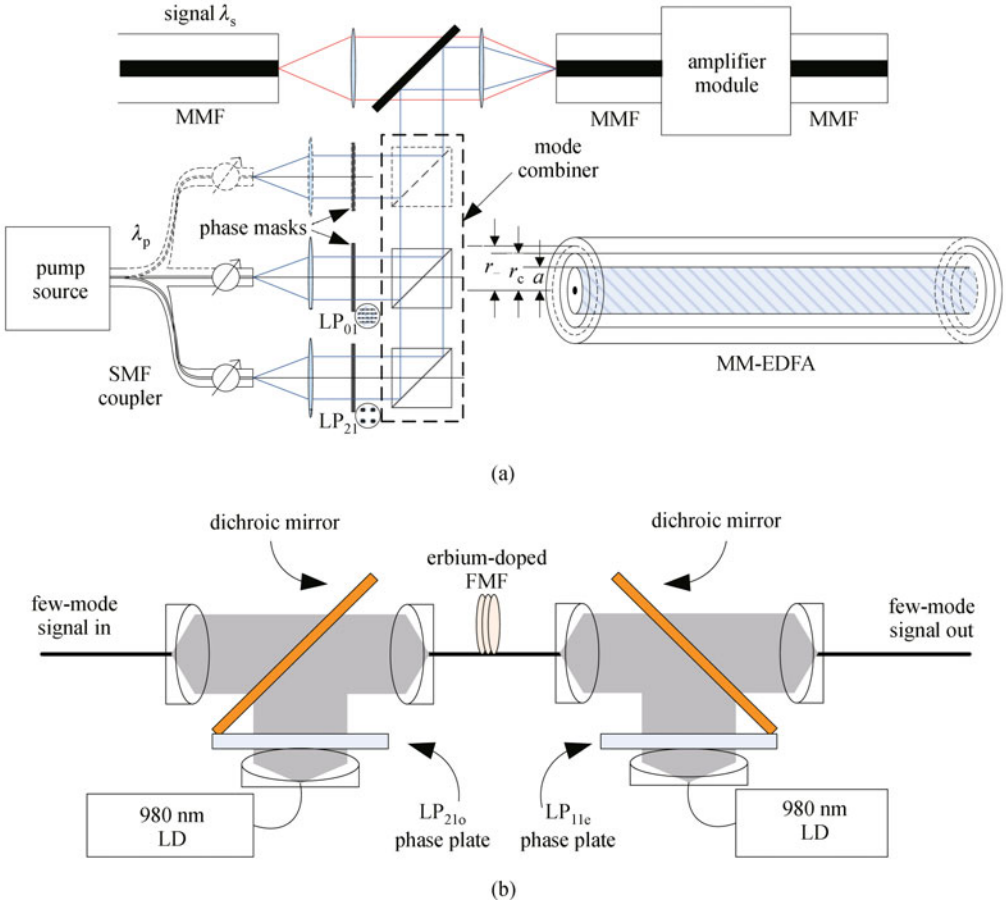

Fig. 1 Theoretical schematic of MM-EDFA (a) and experimental setup of MM-EDFA (b)

$$\frac{\mathrm{d}P_{\mathrm{ASE},i}}{\mathrm{d}z} = P_{\mathrm{ASE},i}\int_0^{2\pi}\int_0^{a} r\mathrm{d}r\mathrm{d}\varphi\ \Gamma_{\mathrm{s},i}(r,\varphi)[N_2(r,\varphi,z)\sigma_{\mathrm{es},i} - N_1(r,\varphi,z)\sigma_{\mathrm{as},i}] + \int_0^{2\pi}\int_0^{a} r\mathrm{d}r\mathrm{d}\phi 2\sigma_{\mathrm{es},i}h\nu_{\mathrm{s}}\Delta\nu N_2(r,\varphi)\Gamma_{\mathrm{s},i}(r,\varphi), \quad (2)$$

$$\frac{\mathrm{d}P_{\mathrm{p},j}}{\mathrm{d}z} = -P_{\mathrm{p},j}\int_0^{2\pi}\int_0^{a} r\mathrm{d}r\mathrm{d}\varphi\ \Gamma_{\mathrm{p},j}(r,\varphi)N_1(r,\varphi,z)\sigma_{\mathrm{ap},j} - \sum_{k=1}^{m_{\mathrm{p}}} d_{\mathrm{p},j\leftrightarrow k}[P_{\mathrm{p},j} - P_{\mathrm{p},k}], \quad (3)$$

where $\Gamma_{\mathrm{s},i}(r,\varphi)$ and $\Gamma_{\mathrm{p},j}(r,\varphi)$ are the normalized intensity profiles of the i-th signal mode and j-th pump mode of the EDF, $P_{\mathrm{s},i}$ and $P_{\mathrm{p},j}$ are their respective powers, $N_1(r,\varphi,z)$ and $N_2(r,\varphi,z)$ are the population densities of Erbium atoms in the lower and upper levels at position (r,φ,z), with $N_1(r,\varphi,z) + N_2(r,\varphi,z) = N_0(r,\varphi)$, the total doping concentration, $\sigma_{\mathrm{as},i}$ and $\sigma_{\mathrm{es},i}$ are the absorption and emission cross-section areas at the i-th signal mode at the wavelength λ_{s}, $\sigma_{\mathrm{ap},j}$ is the absorption cross-section of the j-th pump mode at the wavelength λ_{p}, $\Delta\nu$ is the equivalent amplifying bandwidth, and $d_{\mathrm{s},i\leftrightarrow k}$'s are coupling coefficients between signal modes.

The steady-state population density equations are given by

$$N_1(r,\varphi,z) = \frac{\dfrac{1}{\tau} + \displaystyle\sum_{i=1}^{m_{\mathrm{s}}} \frac{[P_{\mathrm{s},i} + P_{\mathrm{ASE},i}]\sigma_{\mathrm{es},i}\Gamma_{\mathrm{s},i}(r,\varphi)}{h\nu_{\mathrm{s}}}}{\dfrac{1}{\tau} + \displaystyle\sum_{i=1}^{m_{\mathrm{s}}} \frac{[P_{\mathrm{s},i} + P_{\mathrm{ASE},i}](\sigma_{\mathrm{es},i} + \sigma_{\mathrm{as},i})\Gamma_{\mathrm{s},i}(r,\varphi)}{h\nu_{\mathrm{s}}} + \displaystyle\sum_{j=1}^{m_{\mathrm{p}}} \frac{P_{\mathrm{p},j}\sigma_{\mathrm{ap},j}\Gamma_{\mathrm{p},j}(r,\varphi)}{h\nu_{\mathrm{p}}}} N_0(r,\varphi), \quad (4)$$

$$N_2(r,\varphi,z) = \frac{\displaystyle\sum_{i=1}^{m_{\mathrm{s}}} \frac{[P_{\mathrm{s},i} + P_{\mathrm{ASE},i}]\sigma_{\mathrm{as},i}\Gamma_{\mathrm{s},i}(r,\varphi)}{h\nu_{\mathrm{s}}} + \displaystyle\sum_{j=1}^{m_{\mathrm{p}}} \frac{P_{\mathrm{p},j}\sigma_{\mathrm{ap},j}\Gamma_{\mathrm{p},j}(r,\varphi)}{h\nu_{\mathrm{p}}}}{\dfrac{1}{\tau} + \displaystyle\sum_{i=1}^{m_{\mathrm{s}}} \frac{[P_{\mathrm{s},i} + P_{\mathrm{ASE},i}](\sigma_{\mathrm{es},i} + \sigma_{\mathrm{as},i})\Gamma_{\mathrm{s},i}(r,\varphi)}{h\nu_{\mathrm{s}}} + \displaystyle\sum_{j=1}^{m_{\mathrm{p}}} \frac{P_{\mathrm{p},j}\sigma_{\mathrm{ap},j}\Gamma_{\mathrm{p},j}(r,\varphi)}{h\nu_{\mathrm{p}}}} N_0(r,\varphi). \quad (5)$$

Here, ν_{s} and ν_{p} are the signal and pump optical frequencies, τ is the spontaneous emission lifetime for the excited state, m_{s} is total number of guided modes at λ_{s}, m_{p} is total number of guided modes at λ_{p}, h is the Planck constant.

Equations (1)–(5) can be used to calculate the gain and noise figure for all signal modes. Figure 2 shows the gain values of different modes for the FM-EDFA. Figures 2(a) and 2(b) show higher gain for $\mathrm{LP}_{01,\mathrm{s}}$ when pumped by the $\mathrm{LP}_{01,\mathrm{p}}$ and $\mathrm{LP}_{11,\mathrm{p}}$ modes. Conversely, pumping in $\mathrm{LP}_{21,\mathrm{p}}$ results in higher gain for $\mathrm{LP}_{11,\mathrm{s}}$, as shown in Fig. 2(c).

In an experimental study, Yung et al. completed demonstration of a two-mode-EDFA for SDM. The gain for both $\mathrm{LP}_{01,\mathrm{s}}$ and $\mathrm{LP}_{11,\mathrm{s}}$ is over 22 dB and a relatively flat gain profile with a maximum gain variation of 3 dB across the full C-band was also obtained through optimizing active fiber refractive index profile [18]. Yung et al. later extended their work to demonstrate simultaneously amplification of about 20 dB for different spatial-polarization modes ($\mathrm{LP}^{x}_{11,\mathrm{a}}$ and $\mathrm{LP}^{y}_{11,\mathrm{b}}$) [19]. The FM-EDFA, as shown in Fig. 1 (b), was employed in a WDM mode-division multiplexed (MDM) transmission over 50 km of FMF [24].

2.1.2 MC-EDFA

MCF has multiple cores in a single strand of fiber, where each core can only transmit independent information along the fiber. If the cores are completely isolated, the MC-EDFA should have the same properties as the conventional single-mode EDFA with high amplification efficiency and low noise figure. However, there is always residual crosstalk between cores. To optimize amplification performance, the core-to-core cross talk in the MC-EDF should be strictly controlled. In 2011, Abedin et al. demonstrated for the first time a 7-core MC-EDFA, as shown in Fig. 3 [22]. Two tapered fiber bundles (TFB) were used to coupling pump singles and transmission signals into the multi-core EDF. The MC-EDF is specifically designed to match the pitch and mean field diameter (MFD) of the tapered end of the TFB. The advantage of using the TFB is that it is convenient to couple signals in and out of the MCF. However, the disadvantage is that the TFB is difficult to fabricate. Reference [22] reported an average net gain of about 25 dB and an average noise figure of less than 4 dB.

It is noted that the above-mentioned amplifier architec-

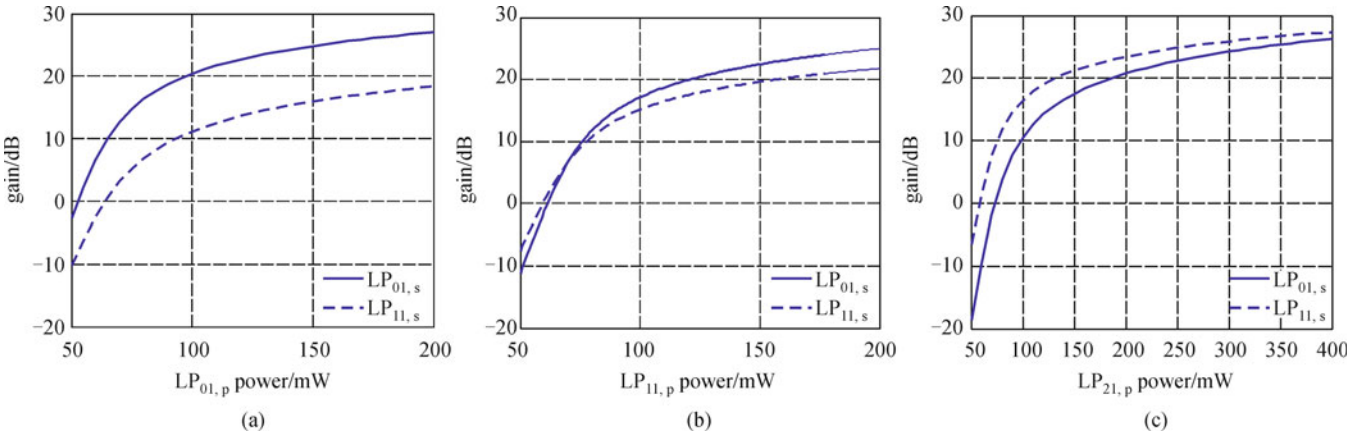

Fig. 2 Modal gain of signal, $LP_{01,s}$ and $LP_{11,s}$, at 1530 nm versus the 980 nm pump power when pump is entirely confined in (a) $LP_{01,p}$, (b) $LP_{11,p}$ and (c) $LP_{21,p}$

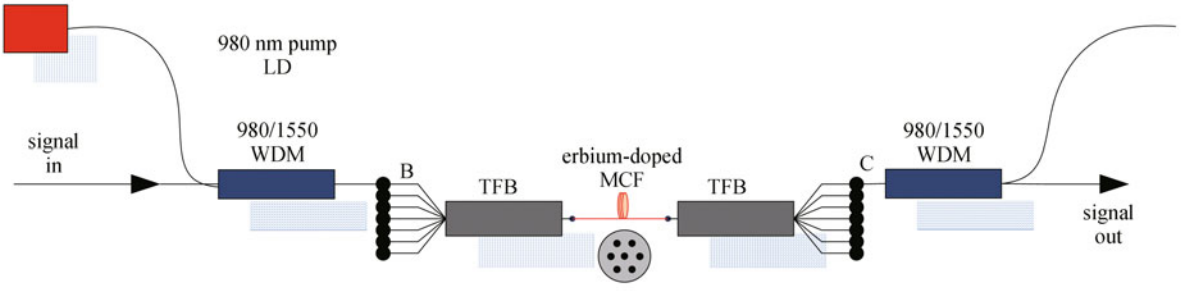

Fig. 3 Experimental setup of 7-core MC-EDFA

ture [22] for MCF is a straightforward approach, where the number of required components is increased by a factor equal to the number of cores (N). Cladding pumped MC-EDFA is being pursued currently. It is expected that cladding-pumped MC-EDFA will have lower power-conversion efficiency than the amplifier in Ref. [22].

An imaging amplification has been proposed to reduce the hardware complexity for MCF EDFAs [25]. A schematic of the imaging amplifier is shown in Fig. 4, in which the signal from the output facet of the MCF or FMF is amplified through a bulk amplifier. Imaging systems (IS 1 and IS 2) are necessary to focus and overlap the beam at the center of the bulk amplifier and couple the signal back to the output fiber. The benefit of this imaging amplifier is that only one amplifier is needed to amplify all signals from many cores, with each core supporting one or several spatial modes. High gain (about 20 dB) and high power conversion efficiency of the imaging amplifier have been obtained in simulations.

2.2 Distributed Raman amplifier (DRA)

Compared with the EDFA, the advantages of DRAs are large optical bandwidth, gain flatness and noise reduction capabilities, while the disadvantages are low gain and low pump efficiency. DRAs are based on stimulated Raman scattering and thus can easily be extended to FMF.

The power evolution for the signal in a DRA is given by

$$\frac{P_{s,m}(z)}{P_{s,m}(0)} = \exp\left[-\alpha_s z + G_m^+(1-e^{-\alpha_p z}) + G_m^- e^{-\alpha_p L}(e^{\alpha_p z}-1)\right], \quad (6)$$

which is a solution to the differential equation governing the evolution of signal in mode m in the undepleted pump approximation. $P_{s,m}$ is the power in signal mode m, α_s and α_p are the absorption coefficients at wavelengths λ_s and λ_p. In Eq. (6), the coefficients $G_m^{\pm}$ describe the mode-dependent exponential gain

$$G_m^+ = \frac{\gamma_R}{\alpha_p}\sum_n f_{n,m} P_{p,n}^+(0), \quad (7)$$

$$G_m^- = \frac{\gamma_R}{\alpha_p}\sum_n f_{n,m} P_{p,n}^-(L), \quad (8)$$

where $P_{p,n}^{\pm}$ is the power in pump mode n, $P_{p,n}^+$ and $P_{p,n}^-$ denote co-propagating and counter-propagating pump, respectively, γ_R is related to the cross section of spontaneous Raman scatting, L is the length of the fiber, and

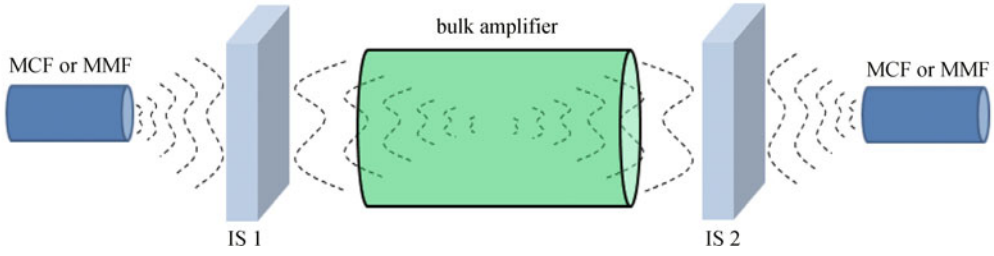

Fig. 4 Schematic of the imaging amplifier where IS is the imaging system

$$f_{n,m} = \frac{\int_{-\infty}^{+\infty}\int_{-\infty}^{\infty} p_n(x,y)p_m(x,y)\mathrm{d}x\mathrm{d}y}{\int_{-\infty}^{+\infty}\int_{-\infty}^{\infty} p_n(x,y)\mathrm{d}x\mathrm{d}y \int_{-\infty}^{+\infty}\int_{-\infty}^{\infty} p_m(x,y)\mathrm{d}x\mathrm{d}y}$$
$$= \int_{-\infty}^{+\infty}\int \Gamma_{s,m}(x,y)\Gamma_{p,n}(x,y)\mathrm{d}x\mathrm{d}y, \quad (9)$$

p_n and p_m are the intensity mode profiles for the signal mode n and the pump mode m, respectively [26].

If signal-spontaneous beat noise is the dominant source of noise added by the amplifier, the noise figure (NF) of the FMF-Roman amplifier can be expressed as [27]

$$NF = \frac{2P^{+}_{\mathrm{ASE},i}(L)}{h\nu\Delta\nu G_{\mathrm{net},i}} + \frac{1}{G_{\mathrm{net},i}}, \quad (10)$$

where $G_{\mathrm{net},i}$ is the net gain of the fiber amplifier.

From Eq. (9), the intensity overlap integrals $f_{n,m}$ can be calculated for the LP pseudomodes. Using Eqs. (6) and (9), the optimization of pump lunch condition can be performed. In 2011, Ryf et al. demonstrated the first FMF Raman amplifier using backward Raman pumping [26]. The mode-equalized distributed Raman gain and equivalent noise figure were 8 dB and −1.5 dB, respectively. In 2012, Ryf et al. investigated performance of FMF Raman amplifiers based on the exact spatial modes of the fiber [28] with a goal of minimizing the mode-dependent gain (MDG) by optimizing the modal pump power distribution. It was concluded that the residual MDG of 0.13 dB can be obtained for each 10 dB of Raman gain.

3 Comparison between FM-EDFA and FM-DRA

The intensity overlap integrals $f_{n,m}$ can be used to compare the quality of the match between signal and pump intensity profile. We calculate the overlap integral of both FM-EDFA, where the wavelength of pump is 980 or 1480 nm, while the wavelength of signal is 1560 nm, and FM-DRA, where the energy is transferred from the pump at λ_p = 1455 nm to the signal at λ_s = 1550 nm [27]. Here, we consider step-index FMF with a core diameter of 8 μm and a numerical aperture of 0.1, same as that in Ref. [20]. It should be noted that the overlap is integrated over the core for EDFA since only the core is active while the overlap is integrated for both the core and cladding for the DRA since both the core and cladding can provide Raman gain. Table 1 summarizes the calculated results.

It is noted that the FM-EDF can support 4 mode groups at the pump wavelength of 980 nm and only 2 mode groups at the wavelength of 1480 or 1455 nm. For pumping using the LP_{01} or LP_{11} modes, the overlapping integrals for 980 nm pumped EDFA are larger than that for the 1455 nm pumped Raman amplifier. Together with larger cross-section, the EDFA is much more efficient. However, the difference between the overlap integrals for the $LP_{01,s}$ and the $LP_{11,s}$ is smaller for the Raman amplifier. Therefore, under these conditions, the MDG for the Raman amplifier is smaller. However, using the 980 nm LP_{21} pump, the overlap integral for the $LP_{11,s}$ signal is greater than that for the $LP_{01,s}$ signal. With the richness in the modal content and two alternative pump wavelengths, the FM-EDFA is expected to be able to achieve the desired MDG more readily than for FM-DRA.

Table 1 Overlap integrals of normalized intensity profile (unit: $10^9 m^{-2}$)

	FM-EDFA (980)		FM-EDFA (1480)		FM-DRA (1455)	
	$LP_{01,s}$	$LP_{11,s}$	$LP_{01,s}$	$LP_{11,s}$	$LP_{01,s}$	$LP_{11,s}$
$LP_{01,p}$	6.1979	3.1954	6.1071	3.2834	6.1967	3.3933
$LP_{11,p}$	4.4043	3.6588	3.4749	3.0603	3.6450	3.3598
$LP_{21,p}$	3.2447	3.4153				
$LP_{02,p}$	4.5764	2.0441				

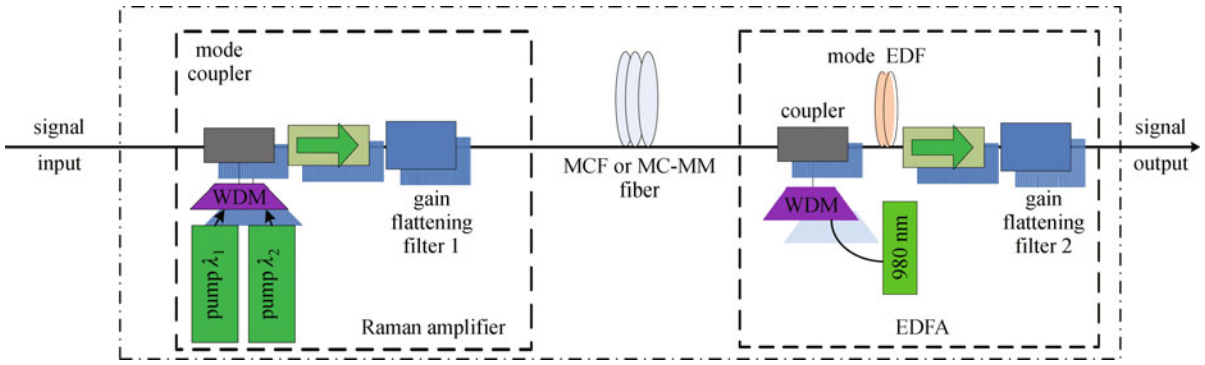

Fig. 5 Hybrid EDF-Raman amplifiers

4 Conclusions

To meet the increased demand of data transport, SDM using FMF or MCF has been proposed and investigated. The functionalities of SDM systems have been successful demonstrated by many research groups. Inline amplifiers are the key to long-distances SDM transmission in MCF or FMF over. Although many reports on optical amplifiers for SDM have been presented, more research and development efforts are needed. As previously mentioned, both EDFA and DRA have pros and cons for SDM. So the best way to amplify the signals in SDM might be the combination of these two techniques, i.e., hybrid amplifiers. Hybrid amplifiers consisting of both functional amplifications, DRA and EDFA (see Fig. 5), might play a significant role for long-haul SDM transmission in the future.

References

1. Richardson D J. Applied physics. Filling the light pipe. Science, 2010, 330(6002): 327–328
2. Mukasa K, Imamura K, Takahashi M, Yagi T. Development of novel fibers for telecoms application. Optical Fiber Technology, 2010, 16 (6): 367–377
3. Imamura K, Mukasa K, Yagi T. Effective space division multiplexing by multi-core fibers. In: Proceedings of European Conference on Optical Commications, 2010, P1.09
4. Zhu B, Taunay T F, Yan M F, Fini J M, Fishteyn M, Monberg E M, Dimarcello F V. Seven-core multicore fiber transmissions for passive optical network. Optics Express, 2010, 18(11): 11117–11122
5. Mukasa K, Imamura K, Tsuchida Y, Sugizaki R. Multi-core fibers for large capacity SDM. In: Proceedings of Optical Fiber Communication Conference, 2011, OWJ1
6. Sakaguchi J, Awaji Y, Wada N, Kanno A, Kawanishi T, Hayashi T, Taru T, Kobayashi T, Watanabe M. 109-Tb/s (7 × 97 × 172-Gb/s SDM/WDM/PDM) QPSK transmission through 16.8-km homogeneous multi-core fiber. In: Proceedings of Optical Fiber Communication Conference and Exposition, 2011, PDPB6
7. Ryf R, Randel S, Gnauck A H, Bolle C, Essiambre R J, Winzer P, Peckham D W, McCurdy A, Lingle R. Space-division multiplexing over 10-km of three-mode fiber using coherent 6 × 6 MIMO processing. In: Proceedings of the National Fiber Optic Engineers Conference and Optical Fiber Communication Conference and Exposition (OFC/NFOEC), 2011, PDPB10
8. Thomsen B C. MIMO enabled 40 Gb/s transmission using mode division multiplexing in multimode fiber. In: Proceedings of National Fiber Communication, 2010, OThM6
9. Franz B, Suikat D, Dischler R, Buchali F, Buelow H. High speed OFDM data transmission over 5 km GI-multimode fiber using spatial multiplexing with 2 × 4 MIMO processing. In: Proceedings of 36th European Conference and Exhibition on Optical Communication (ECOC), 2010, Tu.3.C.4
10. Sakaguchi J, Puttnam B J, Klaus W, Awaji Y, Wada N, Kanno A, Kawanishi T, Imamura K, Inaba H, Mukasa K. Sugisaki R, Kobayashi T, Watanabe M. 19-core fiber transmission of 19 × 100 × 172-Gb/sSDM-WDM-PDM-QPSK signals at 305 Tb/s. In: Proceedings of the National Fiber Optic Engineers Conference, Optical Communication Conference and Exposition (OPF/NFOEC), 2012, PDP5C.1
11. Zhu B, Taunay T F, Fishteyn M, Liu X, Chandrasekhar S, Yan M F, Fini J M, Monberg E M, Dimarcello F V, Abedin K, Wisk P W, Peckham D W, Dziedzic P. Space-, wavelength-, polarization-division multiplexed transmission of 56-Tb/s over a 76.8 km seven-core fiber. In: Proceedings of Optical Fiber Communication Conference (OFC), 2011, PDPB7
12. Salsi M, Koebele C, Sperti D, Tran P, Brindel P, Mardoyan H, Bigo S, Boutin A, Verluise F, Sillard P, Bigot-Astruc M, Provost L, Cerou F, Charlet G. Transmission at 2×100-Gb/s, over two modes of 40 km long prototype few-mode fiber, using LCOS based mode multiplexer and demultiplexer. In: Proceedings of Optical Fiber Communication Conference (OFC), 2011, PDPB9
13. Ryf R, Randel S, Gnauck A H, Bolle C, Sierra A, Mumtaz S, Esmaeelpour M, Burrows E C, Essiambre R J, Winzer P J, Peckham D W, McCurdy A H, Lingle R. Mode-division multiplexing over 96-km of few-mode fiber using coherernt 6 × 6 MIMO processing. Journal of Lightwave technology, 2012, 30(4): 521–531
14. Mears R J, Reekie L, Poole S B, Payne D N. Low-threshold tunable CW and Q-switched fiber laser operating at 1.55 μm. Electronics Letters, 1986, 22(3): 159–160
15. Stacey C D, Jenkins R M, Banerji J, Banerji J, Davies A R.

Demonstration of fundamental mode only propagation in highly multimode fiber for high power EDFAs. Optics Communications, 2007, 269(2): 310–314

16. Krummrich P M. Optical Amplifier for multimode/ multi-core transmission. In: Proceedings of Optical Fiber Communication Conference, 2012, OW1D.1
17. Krummrich P M, Petermann K. Evaluation of potential optical amplifier concepts for coherenct mode multiplexing. In: Proceedings of Optical Fiber Communication Conference, 2011, OMH5
18. Yung Y, Alam S U, Li Z, Dhar A, Giles D, Giles I, Sahu J K, Grüner-Nielsen L, Poletti F, Richardson D J. First demonstration of multimode amplifier for spatial division multiplexed transmission systems. In: Proceedings of 37th European Conference and exhibition on Optical Commications (ECOC), 2011, Th.13.K.4
19. Yung Y, Alam S U, Li Z, Dhar A, Giles D, Giles I, Sahu J K, Poletti F, Richardson D J. Detailed study of modal gain in a multimode EDFA supporting LP_{01} and LP_{11} mode group amplification. In: Proceedings of Optical Fiber Communication Conference, 2012, OM3C.4
20. Bai N, Ip E, Wang T, Li G F.Multimode fiber amplifier with tunable modal gain using a reconfigurable multimode pump. Optics Express, 2011, 19(17): 16601–16611
21. Ip E, Bai N, Huang Y K, Mateo E, Yaman F, Bickham S, Tam H Y, Lu C, Li M J, Ten S, Alan P T L, Tse V, Peng G D, Montero C, Prieto X, Li G. 88 × 3 × 112-Gb/s WDM transmission over 50 km of three-mode fiber with inline few-mode fiber amplifier. In: Proceedings of 37th European Conference and Exhibition on Optical Communication (ECOC), 2011, Th.13.C.2
22. Abedin K S, Taunay T F, Fishteyn M, Yan M F, Zhu B, Fini J M, Monberg E M, Dimarcello F V, Wisk P W. Amplification and noise properties of an erbium-doped multicore fiber amplifier. Optics Express, 2011, 19(17): 16715–16721
23. Nykolak G, Kramer S A, Simpson J R, DiGiovanni D J, Giles C R, Presby H M. An Erbium-doped multimode optical fiber amplifier. IEEE Transactions Photonics Technology Letters, 1991, 3(12): 1079–1081
24. Bai N, Ip E, Huang Y K, Mateo E, Yaman F, Li M J, Bickham S, Ten S, Liñares J, Montero C, Moreno V, Prieto X, Tse V, Chung K M, Lau A P T, Tam H Y, Lu C, Luo Y H, Peng G D, Li G F, Wang T. Mode-division multiplexed transmission with inline few-mode fiber amplifier. Optics Express, 2012, 20(3): 2668–2680
25. Ozdur I, Shu H, Bass M, Li G F. Think outside the fiber: imaging amplifier for space-multiplexed optical transmission. IEEE Photonics Journal, 2012, 4(5): 1316–1324
26. Ryf R, Sierra A, Essiambre R J, Randel S, Gnauck A H, Bolle C, Esmaeelpour M, Winzer P J, Delbue R, Pupalaikise P, Sureka A, Peckham W, McCurdy A, Lingle R Jr. Mode-equalized distributed Raman amplification in 137-km few-mode fiber. In: Proceedings of European Conference and Exposition on Optical Communications (ECOC), 2011, Th.13.K.5
27. Bromage J. Raman amplifier for fiber communication systems. Journal of Lightwave Technology, 2004, 22(1): 79–93
28. Ryf R, Essiambre R, von Hoyningen-Huene J, Winzer P. Analysis of mode-dependent gain in Raman amplified few-mode fiber. In: Proceedings of Optical Fiber Communication Conference (OFC), 2012, OW1D